Registry No. [9,10-$^2H_2$]-18:2$^{\Delta 6,9}$, 111210-15-2; [$^2H_2$]-PiLPC, 111210-16-3; [9,10-$^2H_2$]-18:1$^{\Delta 9}$, 5711-29-5; [9,10-$^2H_2$]-18:2$^{\Delta 6,9}$ methyl ester, 111210-17-4; [9,10-$^2H_2$]-18:2$^{\Delta 6,9}$ ethyl ester *O*-TMS derivative, 111210-18-5.

REFERENCES

Applegate, K. R., & Glomset, J. A. (1986) *J. Lipid Res. 27*, 658–680.

Bitman, J., & Wood, D. L. (1982) *J. Liq. Chromatogr. 5*, 1155–1162.

Bloom, M., Davis, J. H., & Mackay, L. (1981) *Chem. Phys. Lett. 80*, 198–202.

Conner, R. L., Burtness, B., & Ferguson, K. A. (1984) *Lipids 19*, 285–288.

Coolbear, K. P., Berde, C. B., & Keough, K. M. W. (1983) *Biochemistry 22*, 1466–1473.

Crawford, M. A., Hassam, A. G., Williams, G., & Whitehouse, W. (1977) *Adv. Exp. Med. Biol. 83*, 135–143.

Davis, P. J., & Keough, K. M. W. (1983) *Biochemistry 22*, 6334–6340.

Dommes, V., Wirtz-Pietz, F., & Kunau, W. H. (1976) *J. Chromatogr. Sci. 14*, 360–366.

Dratz, E. A., & Deese, A. J. (1986) in *Health Effects of Polyunsaturated Fatty Acids* (Siminopoulous, A. P., Kiefer, R. R., & Martin, R. E., Eds.) pp 319–351, Academic, New York.

Dufourc, E. J., Smith, I. C. P., & Jarrell, H. C. (1984) *Biochemistry 23*, 2300–2309.

Hill, R. J., Prescott, D. J., Spence, S. L., & Conner, R. L. (1983) *Biochim. Biophys. Acta 754*, 150–158.

Kates, M. (1972) in *Techniques* of *Lipidology* (Work, T. S., & Work, E., Eds.) North-Holland, Amsterdam.

Keough, K. M. W., & Davis, P. J. (1979) *Biochemistry 18*, 1453–1459.

Lamptey, M. S., & Walker, B. L. (1976) *J. Nutr. 106*, 86–93.

Morrison, W. R., & Smith, L. M. (1964) *J. Lipid Res. 5*, 600–608.

Neuringer, M., Conner, W. E., Van Patten, C., & Barstad, L. (1984) *J. Clin. Invest. 73*, 272–276.

Perly, B., Dufourc, E. J., & Jarrell, H. C. (1984) *J. Labelled Compd. Radiopharm. 21*, 1–13.

Rance, M., Jeffrey, K. R., Tulloch, A. P., Butler, K. W., & Smith, I. C. P. (1980) *Biochim. Biophys. Acta 600*, 245–262.

Schmitz, B., & Egge, H. (1979) *Chem. Phys. Lipids 25*, 287–298.

Seelig, A., & Seelig, J. (1974) *Biochemistry 13*, 4839–4845.

Seelig, A., & Seelig, J. (1979) *Biochemistry 16*, 45–50.

Seelig, J., & Waespe-Šarčevič, N. (1978) *Biochemistry 17*, 3310–3315.

Shaka, A. J., Keeler, J., & Freeman, R. (1983) *J. Magn. Reson. 52*, 335–341.

Spector, A. A., & Yorek, M. A. (1985) *J. Lipid Res. 26*, 1015–1035.

Stockton, G. W., Johnson, K. G., Butler, K. W., Tulloch, A. P., Boulanger, Y., Smith, I. C. P., Davis, J. H., & Bloom, M. (1977) *Nature (London) 269*, 267–268.

Stubbs, C. D., Kouyama, T., Kinosita, K., Jr., & Ikegami, A. (1981) *Biochemistry 20*, 4257–4262.

Tulloch, A. P. (1979) *Chem. Phys. Lipids 24*, 391–406.

Kinetic Mechanism of DNA Polymerase I (Klenow)†

R. D. Kuchta, V. Mizrahi, P. A. Benkovic, K. A. Johnson, and S. J. Benkovic*

Department of Chemistry, The Pennsylvania State University, University Park, Pennsylvania 16802

Received May 5, 1987; Revised Manuscript Received August 13, 1987

ABSTRACT: The minimal kinetic scheme for DNA polymerization catalyzed by the Klenow fragment of DNA polymerase I (KF) from *Escherichia coli* has been determined with short DNA oligomers of defined sequence. A key feature of this scheme is a minimal two-step sequence that interconverts the ternary KF·DNA$_n$·dNTP and KF·DNA$_{n+1}$·PP$_i$ complexes. The rate is not limited by the actual polymerization but by a separate step, possibly important in ensuring fidelity [Mizrahi, V., Henrie, R. N., Marlier, J. F., Johnson, K. A., & Benkovic, S. J. (1985) *Biochemistry 24*, 4010–4018]. Evidence for this sequence is supplied by the observation of biphasic kinetics in single-turnover pyrophosphorolysis experiments (the microscopic reverse of polymerization). Data analysis then provides an estimate of the internal equilibrium constant. The dissociations of DNA, dNTP, and PP$_i$ from the various binary and ternary complexes were measured by partitioning (isotope-trapping) experiments. The rate constant for DNA dissociation from KF is sequence dependent and is rate limiting during nonprocessive DNA synthesis. The combination of single-turnover (both directions) and isotope-trapping experiments provides sufficient information to permit a quantitative evaluation of the kinetic scheme for specific DNA sequences.

Escherichia coli DNA polymerase I (Pol I)[1] is a multifunctional enzyme involved in the repair and replication of DNA in vivo (Kornberg, 1980). In addition to its reversible polymerase activity that catalyzes the template-directed extension of a primer DNA strand, the enzyme also possesses distinct 3′ → 5′ and 5′ → 3′ exonuclease activities residing on a single 103-kDa polypeptide chain (Jovin et al., 1969). In view of its extensive catalytic repertoire, Pol I has served as a useful model for describing certain enzymatic processes

† This work was supported by NIH Grant 2R01 GM13306-21.

* Author to whom correspondence should be addressed.

[1] Abbreviations: Pol I, *Escherichia coli* DNA polymerase I; KF, Klenow fragment; kDa, kilodalton(s); PP$_i$, inorganic pyrophosphate; dNTP, deoxynucleoside 5′-triphosphate; HPLC, high-pressure liquid chromatography; TEAB, triethylammonium bicarbonate; TEAA, triethylammonium acetate; Tris·HCl, tris(hydroxymethyl)aminomethane hydrochloride; EDTA, ethylenediaminetetraacetic acid.

0006-2960/87/0426-8410$01.50/0

Chart I: DNA Oligomers Used

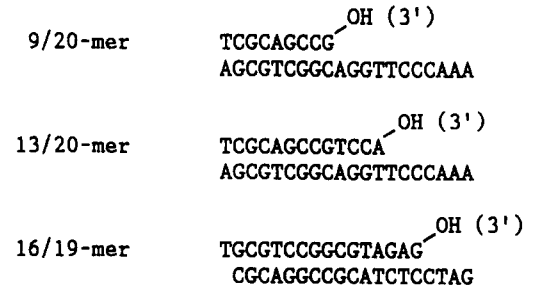

associated with DNA replication. Mechanistic details of the phosphodiester bond-making and bond-breaking reactions catalyzed by the interrelated polymerase and 3′ → 5′ exonulcease activities of Pol I and its large (Klenow) proteolytic fragment (KF) have been elucidated by a variety of stereochemical (Burgers & Eckstein, 1979; Brody & Frey, 1981; Gupta & Benkovic, 1984), structural (Ollis et al., 1985), and kinetic analyses (McClure & Jovin, 1975; Bambara et al., 1976; Bryant et al., 1983; Mizrahi et al., 1985, 1986a).

Steady-state and pre-steady-state kinetic studies have established the important features underlying processive synthesis on alternating copolymer and homopolymer template-primers catalyzed by Pol I and KF. In the present study, isotope-trapping and rapid-kinetic techniques were employed to examine the individual steps involved in KF-catalyzed single nucleotide incorporation and pyrophosphorolysis with a synthetic DNA substrate of defined sequence, and thereby allow some measure of insight into the DNA sequence dependence of the kinetic mechanism.

Experimental Procedures

Materials. Klenow fragment (KF) was purified from *Escherichia coli* CJ155 according to Joyce and Grindley (1983). The *E. coli* strain was kindly provided by Professor C. Joyce. KF concentrations were determined spectrophotometrically with $\epsilon_{278} = 6.32 \times 10^4\ M^{-1}\ cm^{-1}$ (Setlow et al., 1972). T4 polynucleotide kinase was from United States Biochemical Corp. Yeast inorganic pyrophosphatase was from Sigma. [8-^{3}H]dATP was from ICN while all other radioactive compounds were from New England Nuclear. dNTP's were from Sigma. (S_p)-dATPαS was a kind gift of Dr. Jin-Tann Chen. Na_4PP_i (Sigma) was purified by DEAE-Sephadex A-25 column chromatography, elution being with a linear gradient of 0–0.6 M TEAB. PP_i concentrations were determined following pyrophosphatase treatment by the colorimetric phosphate assay of Lanzetta et al. (1979). DE81 and GF/c filters (2.5 cm) were from Whatman. DEAE-Sephadex A-25 was from Pharmacia. Reverse-phase HPLC was performed on a Beckman 421A system equipped with a 25 × 0.46 cm Altex ODS C_{18} column.

Preparation of DNA Duplexes. Oligonucleotides were synthesized on an Applied Biosystems 380A DNA synthesizer. Oligonucleotide duplexes were formed by mixing equimolar template (20-mer) and primer (9-mer or 13-mer) strands (1–50 μM each) in 50 mM NaCl and 15 mM Tris·HCl, pH 7.4. This was boiled for 1 min and then cooled to room temperature over 2–3 h in an oil bath initially set at 65 °C. DNA duplexes are shown in Chart I.

The concentration of 13/20-mer was determined by measuring incorporation of [^{32}P]dAMP. In a total volume of 200 μL, 20–50 nM 13/20-mer, 5 μM [α-^{32}P]dATP (~5000 cpm pmol^{-1}), 0.1 μM KF, 5 mM $MgCl_2$, and 50 mM Tris·HCl, pH 7.4, were incubated at 22 °C. After 2–5 min, 25-μL aliquots were withdrawn and quenched into 12.5 μL of 0.5 M EDTA, pH 7.4. The amount of radioactivity incorporated into DNA was determined by the DE81 filter binding assay. To ascertain that all of the primer was extended, the samples were 5′-^{32}P-end labeled (see below) with [γ-^{32}P]ATP by polynucleotide kinase. Gel electrophoresis revealed that all of the 13/20-mer was converted to 14/20-mer. The concentrations of 9/20-mer and 16/19-mer was determined identically, except the [α-^{32}P]dATP was replaced with [α-^{32}P]dTTP or [α-^{32}P]dGTP, respectively.

DNA Filter Binding Assays. Radioactivity present in DNA was determined according to a previously described DE81 filter binding assay and scintillation counting (Bryant et al., 1983). Samples were mixed with Fisher Scintiverse II and counted on a Beckman LS8100 or LS6800 scintillation counter.

5′-^{32}P-End Labeling. The 5′-^{32}P-end labeling of DNA was performed as described previously (Mizrahi et al., 1986b). If the DNA samples contained EDTA, $MgCl_2$ was added to a final concentration at least 10 mM higher than the EDTA concentration.

Gel Electrophoresis. Denaturing polyacrylamide gel electrophoresis and autoradiography were performed as described previously (Mizrahi et al., 1986b). Gels contained 10–12% acrylamide.

3′-End-Labeled Duplex. A mixture (2 mL) containing 200 nM 13/20-mer duplex, 12.5 mM NaCl, 5 mM $MgCl_2$, 4 μM [α-^{32}P]dATP (~1.4×10^5 cpm/pmol), and 200 nM KF in 50 mM Tris·HCl (pH 7.4) was incubated at 21 °C for 20 min. The reaction was quenched by the addition of EDTA to a concentration of 10 mM. The reaction mix was twice passed through a C18 Sep-Pak (Waters) equilibrated with 15 mM TEAB, pH 7. The Sep-Pak was washed with 10 mL of 7.5% CH_3CN in 15 mM TEAB, pH 7, to elute mononucleotides. Oligonucleotides were then eluted with 10 mL of 35% CH_3CN in 15 mM TEAB, pH 7. Fractions containing ^{32}P-labeled oligonucleotides were found with the DE81 filter binding assay. These were concentrated to 0.4 mL with a Speed-Vac concentrator and injected onto a C18 HPLC column equilibrated with 10% CH_3CN in 0.1 M TEAA, pH 7.0. A 25-min isocratic elution with the equilibration buffer at a flow rate of 1.0 mL/min removed the remaining unreacted mononucleotide. The oligonucleotides were then eluted with a 30-mL linear gradient of 10–21% CH_3CN in 0.1 M TEAA (pH 7.0). The eluant was monitored spectrophotometrically (264 nm) and by liquid scintillation counting. The three peak fractions that correspond to 3′-end labeled 14-mer primer, 20-mer template, and 3′-end labeled 14/20-mer duplex were pooled, lyophilized, and redissolved in 0.12 mL of a solution containing 50 mM NaCl in 15 mM Tris·HCl (pH 7.4). The DNA-containing solution was hybridized as described above. This procedure yielded 60–70% DNA recovery.

The concentration of 3′-[^{32}P]dA-labeled 14/20-mer duplex was determined by measuring the level of incorporation of [^{32}P]dGMP in a polymerization reaction. An aliquot (1 μL) of the hybridized 3′-[^{32}P]dA-labeled 14/20-mer was added to a solution (19 μL) containing 5 mM $MgCl_2$, 5 μM [α-^{32}P]-dGTP (2.5×10^5 cpm/pmol), and 10 μM dTTP in 50 mM Tris·HCl (pH 7.4). Zero points were withdrawn in triplicate prior to initiating polymerization with 10 nM KF. Aliquots were quenched after 1–30 min and assayed for [^{32}P]dGMP incorporation into DNA by the DE81 filter assay. Measurement of the final level of [^{32}P]dGMP incorporation above the background (contributed by the [^{32}P]dAMP label in the 14-mer) allows evaluation of the active 3′-end concentration, assuming the incorporation of three [^{32}P]dGMP residues per available 3′-end (see DNA sequence in Chart I). 3′-[^{3}H]dA-

and 3′-[^{35}S]dA-labeled 14/20-mer were prepared similarly to 3′-[^{32}P]dA-labeled 14/20 mer, except [α-^{32}P]dATP was replaced with either [8-^{3}H]dATP or [α-^{35}S]dATPαS.

Rapid-Quench Polymerization Kinetics. Rapid-quench time points between 20 ms and 3 s were obtained as previously described (Mizrahi et al., 1985). All time points were obtained in duplicate. Polymerization reactions were initiated by mixing equal volumes (20 μL) of KF·DNA and Mg·[^{32}P]dNTP solutions. The KF·DNA solution (1.0 mL) contained 100 nM KF, 300 nM DNA, and 2.5 mM EDTA in 50 mM Tris, pH 7.4. The Mg·[^{32}P]dNTP solution (1.0 mL) contained 4–40 μM [α-^{32}P]dNTP (5000–20 000 cpm pmol^{-1}) and 12.5 mM $MgCl_2$ in 50 mM Tris, pH 7.4. The reactions were quenched into 40 μL of 0.1 or 0.5 M EDTA, pH 7.4, and the amount of radioactivity incorporated into DNA was determined by the filter binding assay. Rapid-quench kinetics of [α-^{35}S]-dATPαS incorporation into 13/20-mer were obtained similarly, except the assays were quenched into 5 mM dithiothreitol and 0.1 M EDTA, pH 7.4.

Single-turnover pyrophosphorolysis reactions were initiated by mixing equal volumes of KF·DNA and Mg·PP_i·dATP solutions and were quenched into 40 μL of 0.1 M EDTA, as above. The stock KF·DNA solutions contained 100 nM 3′-[^{3}H]dA-labeled 14/20-mer duplex (2.9×10^4 cpm/pmol), 800 nM KF, and 2.5 mM EDTA in 50 mM Tris·HCl (pH 7.4). The stock Mg·PP_i·dATP solutions contained 12.5 mM $MgCl_2$, 0.07–0.42 mM PP_i and 10 μM dATP in 50 mM Tris·HCl (pH 7.4). The quenched solutions were assayed for label remaining in the DNA (60 μL) by the DE81 filter binding assay. Single-turnover pyrophosphorolysis of 3′-[^{35}S]dA-labeled 14/20-mer was performed similarly except the assays were quenched into 5 mM dithiothreitol and 0.1 M EDTA, pH 7.4.

Steady-State Polymerization. Steady-state rates of polymerization were measured by incubating 0.2 μM DNA, 1–5 μM [α-^{32}P]dNTP ($\sim$5000 cpm pmol^{-1}), and 5 mM $MgCl_2$ in 50 mM Tris·HCl, pH 7.4, in a final volume of 0.3 mL at 22 °C. Polymerization was initiated by addition of KF to a final concentration of 2 nM. After 15–180 s, 25-μL aliquots were withdrawn and quenched into 12.5 μL of 0.5 M EDTA, pH 7.4. The amount of [^{32}P]dNMP incorporated into DNA was determined by the DE81 filter binding assay. In those cases where several different dNMPs were incorporated into DNA, only one contained ^{32}P.

K_D of DNA. A solution of 50 nM KF, 25–200 nM 13/20-mer, 5 mM $MgCl_2$, and 50 mM Tris·HCl was incubated for 30 s at room temperature. To 40 μL of this solution, 360 μL of 1 μM [α-^{32}P]dATP ($\sim$5000 cpm pmol^{-1}), 5 mM $MgCl_2$, and 50 mM Tris·HCl, pH 7.4, were added. After 15, 30, 45, 60, 75, and 90 s, 50-μL aliquots were withdrawn and added to 25 μL of 0.5 M EDTA, pH 7.4. The amount of radioactivity incorporated into DNA was determined with the filter binding assay and extrapolated to time zero to obtain a measure of enzyme-bound DNA. The amount of enzyme-bound DNA was measured as a function of DNA concentration and the K_D obtained by Scatchard analysis of the data. The K_D of the 9/20-mer was determined similarly, except in addition to 1 μM [α-^{32}P]dATP the second solution also contained 1 μM dTTP and dCTP.

Measurement of the K_D of dATP. KF (50 nM) was incubated for 30 s with 20 nM 13/20-mer and 5 mM EDTA in 50 mM Tris·HCl, pH 7.4. To 40 μL of this mixture, 360 μL of 5 mM $MgCl_2$, 65 nM 9/20-mer, 27–162 nM [α-^{32}P]dATP (1.8×10^5 to 1.1×10^6 cpm pmol^{-1}) and 50 mM Tris·HCl, pH 7.4, were added. At 15-s intervals, 50-μL aliquots were withdrawn and quenched into 25 μL of 0.5 M EDTA, pH 7.4. The amount of [^{32}P]dAMP incorporated into DNA was determined with the filter binding assay. The amount of [^{32}P]DNA at each time was plotted and [^{32}P]dNMP incorporation at time zero determined. From the burst, the K_D was calculated according to eq 4.

Measurement of the K_D of PP_i. KF (50 nM) was incubated for 30 s with 15 nM 3′-[^{32}P]dA-labeled 14/20-mer ($\sim 1.5 \times 10^5$ cpm pmol^{-1}), 5 mM $MgCl_2$, and 50 mM Tris-HCl, pH 7.4. To 40 μL of this solution, 360 μL of 23–230 μM PP_i, 5 mM $MgCl_2$, 1 μM dATP, and 50 μg mL^{-1} heat-denatured calf thymus DNA in 50 mM Tris·HCl, pH 7.4, were added. After 1, 2, 4, 6, 8, and 10 min, 50-μL aliquots were withdrawn and quenched into 25 μL of 0.5 M EDTA, pH 7.4. Radioactivity remaining in DNA was quantitated by the filter-binding assay.

The amount of [^{32}P]DNA remaining at each time was plotted, and the extent of pyrophosphorolysis at time zero was determined. From the amplitude, the K_D was calculated according to eq 5.

Measurement of K_{eq}. KF (100 nM) was incubated with 25 mM 9/20-mer, 0–470 μM PP_i, 0.50 μM dTTP, 2.9 μM dGTP, 5 mM $MgCl_2$, and 50 mM Tris·HCl, pH 7.4, at 22 °C. After 2–5 min, 60-μL aliquots were removed and boiled for 2 min. A portion of each boiled aliquot was 5′-end labeled with ^{32}P, and samples were subjected to gel electrophoresis. The bands corresponding to 9-mer and 10-mer were located by autoradiography of the gel, and the amount of ^{32}P in each band was determined by their excision followed by scintillation counting.

Kinetics for the Measurement of the K_D of dATP and PP_i. The K_D's for dATP and PP_i were determined by observing the partitioning of a KF·DNA complex between dissociation and polymerization or dissociation and pyrophosphorolysis, respectively. The simplest scheme to describe the partitioning of KF·13/20-mer between dissociation and reaction with dATP to form 14/20-mer is

$$\mathrm{KF} + \text{13/20-mer} \overset{k_{off}}{\leftarrow} \mathrm{KF}^{13/20\text{-mer}} \underset{k_{-1}}{\overset{k_1[\mathrm{dATP}^*]}{\rightleftharpoons}} \mathrm{KF}^{13/20\text{-mer}}_{\mathrm{dATP}^*} \underset{k_{-2}}{\overset{k_2}{\rightleftharpoons}}$$

$$\mathrm{KF}^{*14/20\text{-mer}}_{PP_i} \underset{k_{-3}[PP_i]}{\overset{k_3}{\rightleftharpoons}} \mathrm{KF}^{*14/20\text{-mer}} \overset{k_{off}}{\rightarrow} \mathrm{KF} + {}^*14/20\text{-mer}$$

The steps designated with k_2 and k_{-2} represent polymerization and pyrophosphorolysis, respectively. As will be shown later, the rate constant for pyrophosphorolysis, k_{-2}, is very slow. Thus, $k_3 > k_{-2}$ so that under the experimental conditions the polymerization reaction is effectively irreversible. Free KF was trapped with excess 9/20-mer.

The partitioning can be described by a forward net rate constant k_f and a reverse net rate constant k_r (Cleland, 1975; Raushel & Garrard, 1984):

$$k_f = k_1[\mathrm{dATP}]\frac{k_2}{k_{-1} + k_2} \quad (1)$$

$$k_r = k_{off} \quad (2)$$

The amount of 14/20-mer formed is $[k_f/(k_f + k_r)][\mathrm{KF}\cdot 13/20\text{-mer}]$. Given that the rate constant for dissociation of dATP, k_{-1}, is much greater than that for polymerization, k_2 (Bryant et al., 1983), the amount of KF·13/20-mer that reacts to form 14/20-mer is given by eq 3. Upon replacing k_{-1}/k_1

$$[14/20\text{-mer}] = \frac{\frac{k_1k_2}{k_{-1}}[\mathrm{dATP}]}{k_{off} + \frac{k_1k_2}{k_{-1}}[\mathrm{dATP}]}[\mathrm{KF}\cdot 13/20\text{-mer}] \quad (3)$$

with K_D (for dATP dissociation) and rearranging, one obtains

eq 4. Thus, by determining the amount of 14/20-mer formed

$$\frac{1}{[14/20\text{-mer}]} = \frac{1}{[KF\cdot 13/20\text{-mer}]} + \frac{k_{off}K_D^{dATP}}{k_2[dATP]}\frac{1}{[KF\cdot 13/20\text{-mer}]} \quad (4)$$

at various [α-^{32}P]dATP concentrations, the K_D for dATP (K_D^{dATP}) can be determined.

Similarly, partitioning of KF·3′-[^{32}P]dA-labeled 14/20-mer between dissociation and pyrophosphorolysis is described above. Given that the rate constant for dATP dissociation, k_{-1}, is faster than that for polymerization, k_2, and positional isotope exchange experiments with [α,α-$^{18}O_2$]dATP that revealed negligible α,β-bridging → β-nonbridging isotope exchange (Mizrahi et al., 1985), we presume dissociation of PP_i, k_3, is faster than pyrophosphorolysis, k_{-2}. Because the experimental conditions prescribe a large pool of unlabeled dATP, any [α-^{32}P]dATP formed from 3′-[^{32}P]dA-labeled 14/20-mer will not rebind to KF·13/20-mer such that $k_1 \approx 0$. In addition a large excess of heat-denatured calf thymus DNA was included to trap any free KF. Thus, the amount of [α-^{32}P]dATP formed from KF·3′-[^{32}P]dA-labeled 14/20-mer via pyrophosphorolysis is described by eq 5, so that the

$$\frac{1}{[[^{32}P]dATP]} = \frac{1}{KF\cdot{}^*14/20\text{-mer}} + \frac{k_{off}K_D^{PP_i}}{k_{-2}[PP_i]}\frac{1}{KF\cdot{}^*14/20\text{-mer}} \quad (5)$$

K_D of PP_i ($K_D^{PP_i}$) can be determined by measuring the amount of label lost from KF·3′-[^{32}P]dA-labeled 14/20-mer at various concentrations of PP_i.

Haldane Relationship. The Haldane relationship for the ordered conversion of KF·13/20-mer to KF·14/20-mer is described by eq 6. From eq 4 and 5, the K_D's for PP_i and

$$K_{eq} = \frac{K_D(PP_i)}{K_D(dATP)}\frac{k_2}{k_{-2}} \quad (6)$$

dATP are given in eq 7. The value [dATP] is the X intercept

$$K_D^{dATP} = \frac{k_2[dATP]}{k_{off}^{13/20\text{-mer}}} \qquad K_D^{PP_i} = \frac{k_{-2}[PP_i]}{k_{off}^{14/20\text{-mer}}} \quad (7)$$

from the plot of $[dATP]^{-1}$ vs $[14/20\text{-mer}]^{-1}$ according to eq 4. Similarly, the value $[PP_i]$ is the X intercept from the plot of $[PP_i]^{-1}$ vs $[[^{32}P]dATP]^{-1}$ according to eq 5. Thus, by substituting eq 7 into eq 6 we obtain eq 8, where K_{eq} is independent of k_2 and k_{-2} and k_{off} is designated for a given oligomer.

$$K_{eq} = \frac{[PP_i]}{[dATP]}\frac{k_{off}^{14/20\text{-mer}}}{k_{off}^{13/20\text{-mer}}} \quad (8)$$

Computer Simulation. Computer simulations of the kinetics were performed with the program of Barshop et al. (1983), which was kindly provided by Professor C. Frieden. Some data were fit with the program RS 1 (BBN Software Products Corp.).

Results

Incorporation of a single nucleotide into DNA by KF was examined by rapid-quench techniques with a synthetic oligonucleotide duplex (13/20-mer) and dATP (Figure 1). One dAMP is incorporated into each 13/20-mer to form 14/20-mer in a biphasic time course. The rapid initial incorporation of dAMP is stoichiometric with KF and followed by a slow phase with a rate of 0.06 s^{-1}.

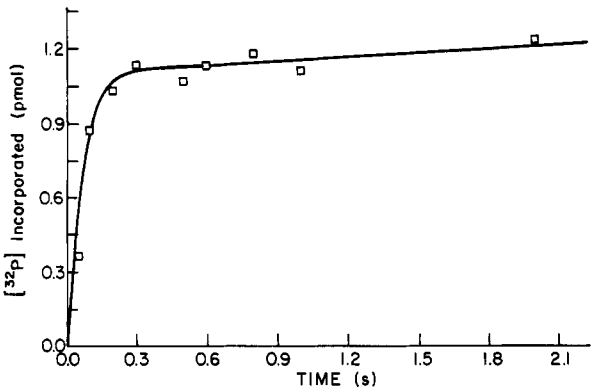

FIGURE 1: Pre-steady-state polymerization on 13/20-mer. The assays were performed as described under Experimental Procedures, except each assay contained 60 nM KF, 510 nM 13/20-mer, and 5 μM [α-^{32}P]dATP. The solid line is the expected time course according to Scheme II.

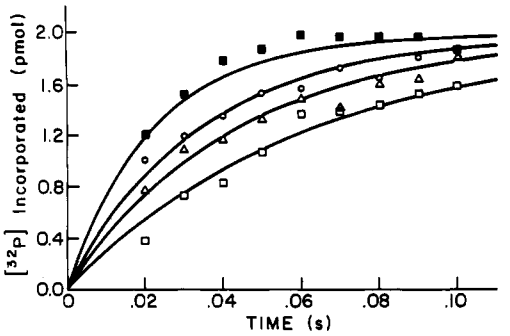

FIGURE 2: Effect of varying dATP concentration on pre-steady-state polymerization. Pre-steady-state polymerization on 13/20-mer was measured with (□) 3.3, (△) 5, (○) 10, and (■) 20 μM [α-^{32}P]dATP. The lines drawn were obtained by fitting the data to the model in the text.

Table I: Dissociation Rates of DNA[a]

substrate/product	rate (s^{-1})
(a) 9/20-mer → 10/20-mer	0.17
(b) 9/20-mer → 12/20-mer	0.17
(c) 9/20-mer → 14/20-mer	0.04
(d) 13/20-mer → 14/20-mer	0.06
(e) 13/20-mer → 17/20-mer	0.30
(f) 16/19-mer → 17/19-mer	0.67

[a] Steady-state polymerization assays were performed as described under Experimental Procedures with the following modifications: (a) 1.0 μM [α-^{32}P]dTTP; (b) 1.0 μM [α-^{32}P]dTTP and 3.3 μM dCTP; (c) 1.0 μM [α-^{32}P]dTTP, 3.3 μM dCTP, and 3.3 μM dATP; (d) 4.0 μM [α-^{32}P]dATP; (e) 4.0 μM [α-^{32}P]dATP and 8.7 μM dGTP; (f) 3.4 μM [α-^{32}P]dGTP.

The effect of varying the dATP concentration on the rate of polymerization is shown in Figure 2. While the slow phase was independent of dATP (data not shown), the rapid phase was not. The data were fit to the model in Scheme I. DNA dissociation is shown as the slow step (0.06 s^{-1}), and as will be demonstrated later, K_D for DNA is 5 nM. Satisfactory fits to the data were obtained by varying k_{obsd} (Figure 2). A secondary plot of k_{obsd}^{-1} vs $[dATP]^{-1}$ revealed that $k_{cat} \approx 50$ s^{-1} and $K_D = 5.5$ μM. To ascertain that the slow step is not binding of 13/20-mer to KF, the experiment was repeated except the 13/20-mer was not preincubated with KF. The rate of dATP incorporation into 13/20-mer was identical whether or not KF·DNA was formed prior to addition of dATP. Finally, manual measurement (see Experimental Procedures) of the steady-state rate of conversion of 13/20-mer to 14/

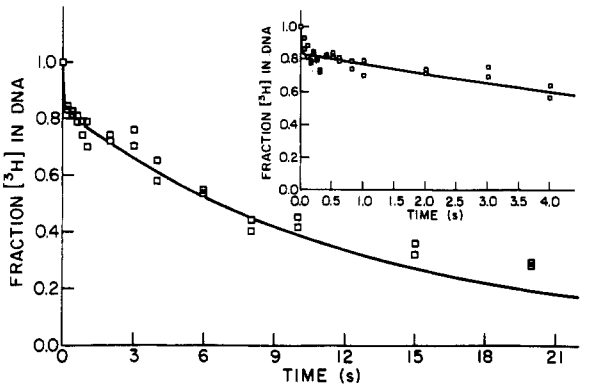

FIGURE 3: Pre-steady-state pyrophosphorolysis was measured as described under Experimental Procedures with 140 μM PP_i. The solid line is the expected time course according to Scheme II.

20-mer under conditions of excess 13/20-mer also yielded a rate of 0.06 s^{-1}, consistent with rate-limiting DNA dissociation.

Scheme I

$$E + 13/20\text{-mer} \underset{0.06\ s^{-1}}{\overset{1.2 \times 10^7\ M^{-1}\ s^{-1}}{\rightleftharpoons}} E{\cdot}13/20\text{-mer} \xrightarrow{k_{obsd}}$$

$$E{\cdot}14/20\text{-mer} \underset{1.2 \times 10^7\ M^{-1}\ s^{-1}}{\overset{0.06\ s^{-1}}{\rightleftharpoons}} E + 14/20\text{-mer}$$

Variation of the DNA sequence caused the steady-state rate of polymerization to change (Table I), indicating that DNA dissociation is sequence dependent. DNA dissociation was further examined by gel electrophoresis of oligomers extended in the presence of various dNTP combinations. The primary product of addition of dATP and dGTP to 13/20-mer is 17/20-mer, the expected product of processive synthesis. The major product formed from 9/20-mer and dTTP, dCTP, and dATP was the expected 14/20-mer, with the steady-state rate of dNTP incorporation set by the rate of dissociation of the KF·14/20-mer complex. These results demonstrate that KF catalyzes processive DNA synthesis on short oligomers with dissociation of DNA occurring only when the required dNTP is missing.

The kinetics of pre-steady-state pyrophosphorolysis were monitored by rapid-quench techniques. Pyrophosphorolysis was initiated by mixing a solution of KF·3′-[^{3}H]dA-labeled 14/20-mer with a Mg·PP_i solution and the time-dependent loss of ^{3}H (as [^{3}H]dATP) from DNA monitored. With 140 μM PP_i, pyrophosphorolysis is biphasic (Figure 3) with the initial phase representing conversion of approximately 17% of the label to [^{3}H]dATP. Rate constants for the fast and slow phases were determined by fitting each phase to an exponential function that gave values >15 s^{-1} and 0.098 (±0.02) s^{-1}, respectively. Reducing the PP_i concentration decreased the magnitude of the initial phase and the rate of the slow phase. We are unable to determine if the initial rate also decreases because of scatter in the data. A reciprocal plot of the rate of the slow phase versus PP_i concentration (not shown) indicated that the K_M of PP_i is approximately 35 μM and k_{cat} is 0.12 s^{-1}.

After each polymerization event, the enzyme must move to read the next template base. If translocation is slower than polymerization, incorporation of the first nucleotide will be faster than later nucleotides. Therefore, the rate of incorporation of two [α-^{32}P]dCTP's into 9/20-mer and 10/20-mer was measured (Figure 4). With 9/20-mer, a dTTP (the 10th base) must be added prior to dCTP addition. In each case, the rate of dCTP incorporation was identical (7.5 s^{-1}). Similar results were also obtained for addition of dGTP to 14/20-mer. The minimum rate of translocation consistent with the data is 45 s^{-1}. Thus, the rate of translocation does not limit processive polymerization, and the rate of polymerization of the first base and latter bases is identical.

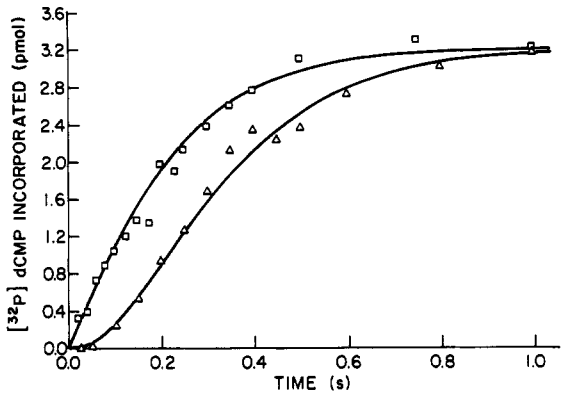

FIGURE 4: Translocation of KF. Standard rapid-quench protocols were used. (□) The 9/20-mer (200 nM) was converted to 10/20-mer by incubating it at 22 °C with 100 nM KF, 14.2 μM dTTP, 2.5 mM $MgCl_2$, and 50 mM Tris, pH 7.4. After 2 min, EDTA was added to a final concentration of 4.3 mM. Assays were initiated by mixing this solution with an equal volume of 12.4 μM [α-^{32}P]dCTP, 12 mM $MgCl_2$, and 50 mM Tris, pH 7.4, and quenched as usual. (△) Assays were initiated by mixing 100 nM KF, 200 nM 9/20-mer, 2 mM EDTA, and 50 mM Tris, pH 7.4, with an equal volume of 12.4 μM dTTP, 12.4 μM [α-^{32}P]dCTP, 12 mM $MgCl_2$, and 50 mM Tris, pH 7.4, and quenched as usual. The lines were obtained by fitting the data to the model shown below. D represents 9/20-mer and DT, DTC, and DTCC represent the DNA product after addition of one, two, and three nucleotides to the 9/20-mer. The rates of polymerization (k_{pol}) and translocation (k_t) were assumed to be identical for each polymerization and translocation step, respectively.

$$E{\cdot}D \xrightarrow[(dTTP)]{k_{pol}} E'{\cdot}DT \xrightarrow{k_t} E{\cdot}DT \xrightarrow[(dCTP)]{k_{pol}} E'{\cdot}DTC \xrightarrow{k_t} E{\cdot}DTC \xrightarrow[(dCTP)]{k_{pol}} E'{\cdot}DTCC$$

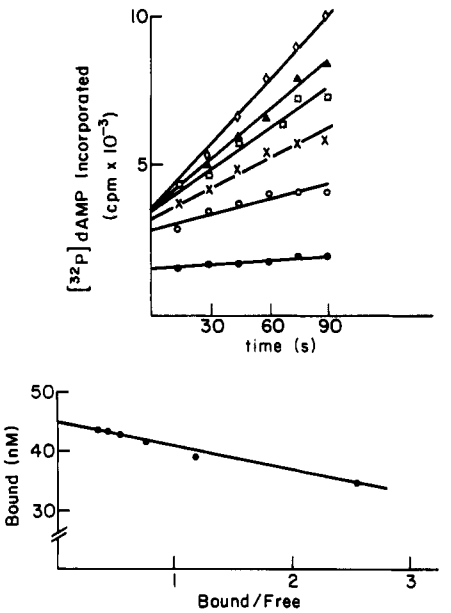

FIGURE 5: Scatchard plot of the amount of KF·13/20-mer formed as a function of DNA concentration. Experimental conditions were as described under Experimental Procedures. The upper panel shows the amount of [α-^{32}P]dATP incorporated into DNA with 48 (●), 72 (○), 96 (×), 120 (□), 144 (▲), and 168 nM 13/20-mer (◇). The amount of ^{32}P incorporated into DNA at time zero (a measure of enzyme bound DNA) was determined, and the data were then subjected to Scatchard analysis (lower panel) to determine the K_D.

Substrate and Product Binding. Binding of DNA to KF was measured by forming a KF·DNA complex at various concentrations of DNA and then diluting it into a solution containing the next correct [^{32}P]dNTP. The [^{32}P]dNTP concentration was sufficient to trap all of the KF·DNA. Therefore, the amount of KF·DNA present in the preincu-

bation is equal to the quantity of [^{32}P]dNTP incorporated into DNA in the first turnover. This is obtained by extrapolation of the measured [^{32}P]DNA to zero time (Figure 5). Scatchard analysis of the data (insert) yields a K_D of 5 nM for 13/20-mer in which 1 mol of DNA is bound per mole of KF at saturation. Similarly, the K_D of 9/20-mer is 4.5 nM. Omitting Mg^{2+} from the preincubation did not affect the K_D.

Substrate dNTP binding was examined with 13/20-mer and dATP. KF·DNA was formed and diluted into solutions containing various amounts of [^{32}P]dATP. The amount of [^{32}P]dAMP incorporated into the DNA is dependent upon the K_D of dATP, the rate of dAMP incorporation (k_{cat}, which is k_2 in eq 1–4), and the dissociation rate of KF·DNA (k_{off}) (see Experimental Procedures). As shown earlier, $k_{cat} = 50\ s^{-1}$ and k_{off} is probably between 0.06 and 0.17 s^{-1}. Half-maximal [^{32}P]dAMP incorporation occurs at 21 nM [α-^{32}P]dATP, so that K_D(dATP) = 6–17 μM.

The binding of PP_i to KF was measured similarly to dNTP binding, except that the DNA used was 3′-[^{32}P]dA-labeled 14/20-mer (data not shown). Pyrophosphorolysis results in loss of [^{32}P] (as [α-^{32}P]dATP) from the DNA. Omission of PP_i resulted in no loss of label from 14/20-mer, indicating that the 3′ → 5′ exonuclease did not hydrolyze any DNA under the experimental conditions. As shown earlier, k_{cat} (this is k_{-2} in eq 5) for pyrophosphorolysis is 0.12 s^{-1}, and the dissociation rate of KF·14/20-mer is 0.06 s^{-1}. Half of the label is lost at 46 μM PP_i, so $K_D(PP_i) \approx 100\ \mu M$.

Equilibrium Constant. The equilibrium constant (K_{eq}) for 9/20-mer + dTTP ⇌ 10/20-mer + PP_i was measured by incubating 9/20-mer, dTTP, and PP_i and determining the amount of 9/20-mer and 10/20-mer present when equilibrium was reached. Several precautions were observed in order to ensure the validity of the measurement. When PP_i was omitted from the reaction, all 9/20-mer was converted to 10/20-mer, indicating all the DNA can be elongated. The reactions were run for 2–5 min at each PP_i concentration. The value of K_{eq} did not vary with time, suggesting that equilibrium was attained within 2 min. Finally, dGTP (the 3′-terminal residue of the 9-mer) was included in the reaction. If the primer 3′-terminus (dGMP) was removed by either pyrophosphorolysis or 3′ → 5′ exonuclease activity, KF should rapidly replace it using the added dGTP. Gel electrophoresis revealed less than 5% of the primer 9-mer was converted to 8-mer. Determination of K_{eq} at three PP_i concentrations gave a value of 513 ± 65.

Phosphorothioate Elemental Effects. Recently it was found that replacement of dNTP with dNTPαS results in V_{max} elemental effects of 1.6 on polymerization and 18 on pyrophosphorolysis with poly[d(AT)] as substrate (Mizrahi et al., 1985). The large difference in elemental effects was ascribed in part to a change in K_{eq} for the reaction. These observations were reexamined by measuring polymerization and pyrophosphorolysis with 13/20-mer as substrate. Pre-steady-state incorporation of dATPαS into 13/20-mer was 3-fold slower than dATP incorporation under V_{max} conditions and 7-fold slower under V_{max}/K_M conditions (not shown). Steady-state incorporation, which is governed by the dissociation rate of product 14/20-mer, was reduced 5-fold upon replacement of dATP with dATPαS. Loss of label from 3′-[^{35}S]dA-labeled 14/20-mer via pyrophosphorolysis was examined at 140 μM PP_i. There was no detectable burst, and the rate of pyrophosphorolysis was 43-fold slower than the rate with nonphosphorothioate-containing 14/20-mer. Under equilibrium conditions similar to those used for dTTP, K_{eq} for the reaction

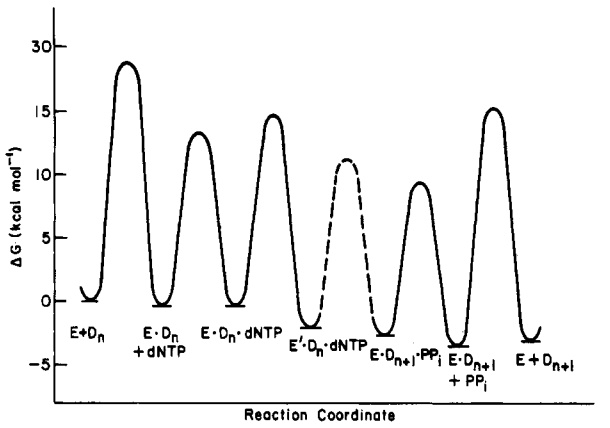

FIGURE 6: Gibbs free energy profile for the reaction catalyzed by DNA Pol I with a standard state of 5 nM DNA (D_n and D_{n+1}), 5 μM dNTP, and 20 μM PP_i.

9/20-mer + dTTPαS ⇌ 10/20-mer + PP_i is approximately 19 000, 37-fold greater than K_{eq} for dTTP.[2]

Discussion

The kinetic mechanism of the polymerase activity of the Klenow fragment has been investigated with a random sequence DNA template-primer. The minimal mechanism consistent with the results of this study is shown in Scheme II, and the corresponding energy profile is illustrated in Figure 6. The experimental steps leading to its construction are now reviewed.

Scheme II

$$E + D \underset{}{\overset{K_D = 5\ nM}{\rightleftharpoons}} E{\cdot}D \overset{K_D^{dATP} = 5\ \mu M}{\rightleftharpoons} E{\cdot}D{\cdot}dATP \underset{0.5\ s^{-1}}{\overset{50\ s^{-1}}{\rightleftharpoons}} E'{\cdot}D{\cdot}dATP \overset{K \approx 2.5}{\rightleftharpoons} E'{\cdot}DA{\cdot}PP_i \overset{K_D^{PP_i} = 100\ \mu M}{\rightleftharpoons}$$

$$E{\cdot}DA \underset{0.06\ s^{-1}}{\overset{1.2 \times 10^7\ M^{-1}\ s^{-1}}{\rightleftharpoons}} E + DA$$

The catalytic competence of the E·DNA complex that was previously demonstrated with a poly(dA)·oligo(dT) template-primer substrate (Bryant et al., 1983) is equally applicable to the synthetic 13/20-mer substrate. This property was exploited for the purpose of evaluating the binding constant of the binary complex formed between KF and the 13/20-mer as well as those of dATP and PP_i for the KF·DNA complex by means of standard isotope-trapping techniques.

Rapid-quench techniques then were employed to examine individual steps involved in single nucleotide polymerization and pyrophosphorolysis. The rapid dATP incorporation observed in pre-steady-state polymerization (50 s^{-1}) occurs at a somewhat faster rate than the rate of processive polymerization on poly(dA)·oligo(dT) (6–14 s^{-1}; Mizrahi et al., 1985; McClure & Jovin, 1975). The small elemental effect on the polymerization reaction indicates that a step other than chemical bond formation is rate limiting, in accordance with results obtained with poly(dA)·oligo(dT) (Mizrahi et al., 1985). In the absence of evidence to the contrary, this step remains assigned to a conformational change of the ternary KF·DNA·dNTP complex to a form posed for nucleophilic displacement.

Confirmatory evidence for the importance of this step was obtained by studying single turnover pyrophosphorolysis of the

[2] This value of K_{eq} is subject to substantial experimental error. Optimal measurement of K_{eq} occurs with conversion of approximately 50% of the 9/20-mer to 10/20-mer. However, at the concentrations of PP_i predicted to give 50% conversion (11.5 mM PP_i, assuming $K_{eq} \approx 19000$), KF is inhibited >95% by the PP_i.

14/20-mer. The biphasic kinetic data are consistent with a sequence where a rapid step precedes a slow first-order process.[3] As illustrated in Scheme II, these steps are assigned to a rapid phosphodiester bond cleavage step and a slow conformational change of the resultant KF·dATP·13/20-mer complex to a form from which dATP can dissociate. By correcting the amount of label lost from 14/20-mer during the fast phase with 140 μM PP_i for the fact that the PP_i is not saturating (K_D = 100 μM), the internal equilibrium constant of the chemical step is calculated to be approximately 2.5 ($\Delta G \approx 0.5$ kcal mol^{-1}) in favor of the polymerization reaction. The observed rate of pyrophosphorolysis at saturating PP_i (0.12 s^{-1}) is somewhat less than the rate predicted from the minimal kinetic scheme (0.2 s^{-1}). This is likely a reflection of experimental uncertainty in the measurements.

The rate of steady-state polymerization on the 13/20-mer (0.06 s^{-1}) is much slower than the pre-steady-state rate (50 s^{-1}). This contrasts with the observation that pre-steady-state and steady-state processive polymerization of poly(dA)·oligo(dT) are identical (Mizrahi et al., 1985). Since the polymerization reaction on 13/20-mer is limited to one nucleotide by omission of the next correct dNTP, the steady-state rate is limited by the dissociation rate of KF·DNA. Rate-limiting DNA dissociation was observed with every oligomer tried when the following correct dNTP was omitted. During processive DNA synthesis, however, inclusion of the next correct dNTP allows translocation to the next polymerization site at a rapid rate ($k_{trans} > 45$ s^{-1}) followed by incorporation of the next nucleotide, thereby avoiding the slow KF·DNA dissociation step.

Both binding and the dissociation rate of DNA from KF are sequence dependent. The K_D for 9/20-mer and 13/20-mer is 5 nM. This is similar to that observed with poly[d(AT)] (McClure & Jovin, 1975) but is much lower than the K_D observed for poly(dA)·oligo(dT) (200 nM; Bryant et al., 1983). The rate of DNA dissociation varied 10-fold (0.06–0.67 s^{-1}) as the DNA was varied. In addition to sequence effects, these results may reflect the effect of a shortened template overhang in the cases of 17/20-mer and 17/19-mer products (Table I). This sequence specificity is consistent with the recent results on KF-catalyzed idling turnover on two different DNAs (Mizrahi et al., 1986b).

Direct measurement of the equilibrium constant for the reaction 9/20-mer + dTTP → 10/20-mer + PP_i gives a value of 510 ± 60. This is very close to that estimated from the steady-state kinetic parameters for Pol I catalyzed polymerization with poly[d(AT)] as the DNA substrate (500 ± 100; McClure & Jovin, 1975). The external K_{eq} for the reaction in Scheme II is also given by the Haldane relationship:

$$K_{eq} = \frac{K_D^{PP_i}}{K_D^{dATP}} \frac{k_{cat}(\text{polymerization})}{k_{cat}(\text{pyrophosphorolysis})}$$

Due to the methods used to measure the K_D's of PP_i and dATP, this reduces to eq 8a (see Experimental Procedures):

$$K_{eq} = \frac{[PP_i]}{[dATP]} \frac{k_{off}^{DNA_{n+1}}}{k_{off}^{DNA_n}} \quad (8a)$$

The terms $k_{off}^{DNA_{n+1}}$ (0.06 s^{-1}), [PP_i] (46 μM), and [dATP] (21 nM) are experimentally determined values. The value of k_{off} cannot be experimentally measured but is probably between 0.06 and 0.17 s^{-1} (Table I), so that K_{eq} = 790–2200, in fair agreement with the measured value of 500.

A previous study found that replacment of dNTP with dNTPαS resulted in an elemental effect ($k_{dATP}/k_{dATP\alpha S}$) of 1.6 on polymerization and 18 on pyrophosphorolysis with poly[d(AT)] as substrate (Mizrahi et al., 1985). Similar nonequivalent elemental effects are observed with 13/20-mer as substrate. At least part of the difference can be ascribed to the approximately 37-fold increase in K_{eq} upon replacement of dNTP with dNTPαS. This change in K_{eq} is consistent with the fact that the secondary structure of the DNA is altered upon incorporation of phosphorothioate-containing nucleotides, as evidenced by a lowering of its melting temperature (Eckstein & Jovin, 1983). In addition to decreasing the rate of phosphodiester bond formation, dNTPαS substitution also reduces the dissocation rate of the phosphorothioate-containing DNA product. The affected step could be either the actual DNA dissociation step or a nonchemical step that is required for DNA dissociation. If this step occurs after polymerization but before PP_i release, it would also result in a larger elemental effect on pyrophosphorolysis than on polymerization. In sum, these results demonstrate that with reactions such as DNA polymerization, phosphorothioate substitution can affect processes other than chemical bond formation owing to its perturbation of DNA secondary structure.

The single nucleotide incorporation and pyrophosphorolysis studies presented here have allowed insights into the steps governing the mechanism of Pol I, which are ordinarily obscured by the presence of the following complementary nucleotide substrates. This has permitted the elucidation of a complete kinetic scheme for Pol I catalyzed polymerization that accurately predicts both the polymerization and pyrophosphorolysis reactions (see Figures 1 and 3). The key features of this scheme are that the external equilibrium (500) is only partially reflected in the chemical step (internal equilibrium = 2.5) and the rate-determining step is a conformational change that precedes catalysis. The role of this conformational change is unknown. Ferrin and Mildvan (1986) showed that in several enzyme–template–substrate complexes the relative affinities for complimentary and noncomplimentary substrates are unaffected by the template. They speculated that this step involves the enzyme-bound Mg^{2+} changing from binding solely to the γ-phosphate of the incoming dNTP to binding both the β- and γ-phosphates. This conformational change may also be the process by which Pol I distinguishes between correct and incorrect dNTP's. Experiments to elucidate this point are in progress.

The free energy profile of the reaction catalyzed by Pol I is shown in Figure 6. The dashed line represents an upper limit on the activation barrier for the chemical polymerization step. Pol I is similar to the calcum-transporting ATPase (Pickart & Jencks, 1984), mitochondrial F1 ATPase (Penefsky, 1985), and myosin (Adelstein & Eisenberg, 1983) where the internal equilibrium is near unity so that the free energy change of ATP hydrolysis is expressed in binding of substrates and products. At the other extreme is dihydrofolate reductase (Fierke et al., 1987), where most of the free energy change is expressed during the chemical step. Triosephosphate isomerase is in-

[3] We considered the possibility that the observed biphasic pyrophosphorolysis kinetics are due to two forms of KF-bound PP_i that are in equilibrium. Consequently, the amplitude of the rapid phase is determined by the equilibrium between the two forms while their rate of interconversion (k_c) determines the slow phase (0.1 s^{-1}):

$$KF^{PP_i}_{DNA_n} \underset{k_{-c}}{\overset{k_c}{\rightleftharpoons}} KF'^{PP_i}_{DNA_n} \xrightarrow{k_{cat}^{PP_i}} \text{products}$$

In order to account for the observed amplitude of the rapid phase, the equilibrium between the two forms must be approximately 3–5, so that k_{-c} = (3–5) × 0.1 s^{-1} or 0.3–0.5 s^{-1}. This value for k_{-c} is 100-fold too slow to accommodate the observed rate of polymerization (50 s^{-1}), thus excluding this model.

termediate between these extremes (Albery & Knowles, 1976). With Pol I, most of the free energy change occurs in the rate-determining conformational change whereby the enzyme "selects" the correct dNTP. Thus, Pol I is similar to the ATPases in that both couple the favorable free energy of catalysis to a separate process—the ATPases caalyze coupled vectorial processes to do mechanical work (Jencks, 1980), while Pol I couples the favorable free energy change to a process that helps ensure the fidelity of DNA replication.

ACKNOWLEDGMENTS

The expert assistance of Dwayne Allen and Mark Young is most gratefully acknowledged.

REFERENCES

Adelstein, R. S., & Eisenberg, E. (1980) *Annu. Rev. Biochem. 49*, 921.
Albery, W. J., & Knowles, J. R. (1976) *Biochemistry 15*, 5627.
Bambara, R. A., Uyemura, D., & Lehman, I. R. (1976) *J. Biol. Chem. 251*, 4090.
Barshop, B. A., Wrenn, R. F., & Frieden, C. (1983) *Anal. Biochem. 130*, 134.
Brody, R. S., & Frey, P. A. (1981) *Biochemistry 20*, 1245.
Bryant, F. R., Johnson, K. A., & Benkovic, S. J. (1983) *Biochemistry 22*, 3537.
Burgers, P. M. J., & Eckstein, F. (1979) *J. Biol. Chem. 254*, 6889.
Cleland, W. W. (1975) *Biochemistry 14*, 3220.
Eckstein, F., & Jovin, T. M. (1983) *Biochemistry 22*, 4546.
Ferrin, L. J., & Mildvan, A. S. (1986) *Biochemistry 25*, 5131.
Fierke, C. A., Johnson, K. A., & Benkovic, S. J. (1987) *Biochemistry 26*, 4085.
Gupta, A. F., & Benkovic, S. J. (1984) *Biochemistry 23*, 5874.
Jencks, W. P. (1983) *Adv. Enzymol. Related Areas Mol. Biol. 51*, 75.
Jovin, T. M., Englund, P. T., & Bertsch, L. L. (1969) *J. Biol. Chem. 244*, 2996.
Joyce, C. M., & Grindley, N. D. F. (1983) *Proc. Natl. Acad. Sci. U.S.A. 80*, 1830.
Kornberg, A. (1980) *DNA Replication*, Freeman, San Francisco.
Lanzetta, P. A., Vlvarez, L. J., Reinach, P. S., & Candia, O. A. (1979) *Anal. Biochem. 100*, 75.
McClure, W. R., & Jovin, T. M. (1975) *J. Biol. Chem. 250*, 4073.
Mizrahi, V., Henrie, R. N., Marlier, J. F., Johnson, K. A., & Benkovic, S. J. (1985) *Biochemistry 24*, 4010.
Mizrahi, V., Benkovic, P. A., & Benkovic, S. J. (1986a) *Proc. Natl. Acad. Sci. U.S.A. 83*, 231.
Mizrahi, V., Benkovic, P., & Benkovic, S. J. (1986b) *Proc. Natl. Acad. Sci. U.S.A. 83*, 5769.
Ollis, D. L., Brick, P., Hamlin, R., Xuong, N. G., & Steitz, T. A. (1985) *Nature (London) 313*, 762.
Penefsky, H. S. (1985) *J. Biol. Chem. 260*, 13728.
Pickart, C. M., & Jencks, W. P. (1986) *J. Biol. Chem. 259*, 1629.
Raushel, F. M., & Garrard, L. J. (1984) Biochemistry *23*, 1791.
Setlow, P., Brutlag, D., & Kornberg, A. (1972) *J. Biol. Chem. 247*, 224.

N-Methyltransferase Function of the Multifunctional Enzyme Enniatin Synthetase†

Andreas Billich and Rainer Zocher*

Institut für Biochemie und Molekulare Biologie der Technischen Universität Berlin, 1000 Berlin 10, West Germany

Received May 19, 1987; Revised Manuscript Received August 3, 1987

ABSTRACT: The *N*-methyltransferase function of the multifunctional enzyme enniatin synthetase was studied. Similar to other transmethylases, *S*-adenosyl-L-homocysteine (AdoHcy) and sinefungin were found to be potent inhibitors of the *S*-adenosylmethionine-dependent reaction. The K_m value was found to be 10 μM, and the K_i values for AdoHcy and sinefungin were 4 and 110 μM, respectively. Sinefungin acted as a competitive inhibitor with respect to *S*-adenosyl-L-methionine (AdoMet), whereas AdoHcy exhibited an inhibition pattern characteristic for a partial competitive inhibitor. This indicates that AdoHcy does not directly compete with AdoMet but binds to a discrete inhibitory site. In addition, AdoHcy inhibited the formation of the unmethylated depsipeptide formed in the absence of AdoMet. In contrast, sinefungin exhibited no influence on the synthesis of demethylenniatin. This finding confirms the assumption that two different binding sites for the inhibitors must be present. Like other methyltransferases, enniatin synthetase can be affinity labeled by UV irradiation of the protein in the presence of AdoMet labeled at the methyl group. The photoreaction was shown to be site specific, and a binding stoichiometry of one methyl group per enzyme molecule was observed. Limited proteolysis of the methyl-labeled enzyme yielded besides a number of unlabeled fragments only one radiolabeled fragment, size 25 kDa, obviously containing the binding site for AdoMet. Evidence was obtained that the binding site for valine, the substrate to be methylated, was not present on this fragment.

A peculiar property of many peptides from the secondary metabolism of fungi and actinomycetes is the occurrence of methylated peptide bonds in these molecules, as in the case of, e.g., cyclosporins, destruxins, enniatins, actinomycins, and quinoxaline antibiotics. These peptides or depsipeptides, which often contain unusual amino acids not present in proteins, are synthesized via nonribosomal pathways (Kleinkauf & von Döhren, 1981). The enzyme systems responsible for the formation of these metabolites obviously exhibit an *N*-methyltransferase function since in no case were N-methylated

† This work was supported by the Deutsche Forschungsgemeinschaft (Sonderforschungsbereich 9, Teilprojekt C 3).

* Author to whom correspondence should be addressed.

0006-2960/87/0426-8417$01.50/0